Agricultural and Forest Meteorology 214-215 (2015) 319–327

Contents lists available at ScienceDirect

Agricultural and Forest Meteorology

journal homepage: www.elsevier.com/locate/agrformet

Hysteresis loops between canopy conductance of grapevines and meteorological variables in an oasis ecosystem

Yan Bai[a], Gaofeng Zhu[a,*], Yonghong Su[b], Kun Zhang[a], Tuo Han[a], Jinzhu Ma[a], Weizhen Wang[b], Ting Ma[a], Lili Feng[a]

[a] Key Laboratory of Western China's Environmental Systems (Ministry of Education), College of Earth and Environmental Sciences, Lanzhou University, Lanzhou 730000, China
[b] Cold and Arid Regions Environmental and Engineering Research Institute, Chinese Academy of Science, Lanzhou 730000, China

ARTICLE INFO

Article history:
Received 13 April 2015
Received in revised form 21 August 2015
Accepted 25 August 2015
Available online 8 September 2015

Keywords:
Sap flow
Canopy transpiration
Canopy conductance
Diurnal courses
Hysteresis loops
Grapevines

ABSTRACT

Canopy conductance (g_c) is a key parameter that determines plant transpiration rate, and it is sensitive to multiple environmental variables. The relationships between g_c and micrometeorological variables still need to be investigated across a wide range of biomes and climatic conditions. In this study, sap flow, micrometeorological and biological factors for a vineyard at an oasis in Northwest China were measured from July to September in 2013 and 2014. Values of g_c were calculated from the simplified Penman–Monteith equation, and diurnal patterns of g_c were investigated in two study years. The relationships between g_c and main micrometeorological variables (global radiation R, vapor pressure deficit D, air temperature T) during the day exhibited hysteresis loops. By dividing daytime into three time periods, it was found that in the first period (7:00–11:00), stomatal opened quickly as R, D and T increase, so g_c increased positively to increasing R, D and T. In the second period (11:00–17:00), followed by stomatal closure, g_c decreased negatively to increasing R, D and T. In the third period (17:00–21:00), as stomatal aperture kept decreasing until sunset, g_c decreased positively to decreasing R, D and T. A simple linear model was used to simulate variations in g_c for the first period and the third period, and a negative logarithmic model was used for the second period. These models were consistent in predicting daytime variations in g_c. The results are useful in improving our current understanding of relationships between plant physiological and environmental processes in the oasis ecosystem.

1. Introduction

Plant transpiration (E_c) is a subject of increasing research interest (Lagergren and Lindroth, 2002; Buckley et al., 2012), especially in regions where transpiration is a fundamental datum in understanding the ecophysiology of plants (Chang et al., 2014). Jasechko et al. (2013) reported that transpiration is by far the largest water flux from earth's continents, representing 80–90% of terrestrial evapotranspiration (*ET*). Considering the dominance of E_c in continental *ET*, future changes in E_c will have significant impacts on global land temperatures and the fraction of precipitation entering rivers (Jasechko et al., 2013).

Canopy conductance (g_c) plays a key role in gas and energy exchanges across vegetated surfaces via their direct controls on CO_2 uptake and water losses (Alfieri et al., 2008; Berry et al., 2010; Damour et al., 2010; Ono et al., 2013). Therefore, studying the responses of g_c to the environmental variables is essential to understand the relationships between the plant physiological and environmental processes (Daly et al., 2004; Kumar et al., 2011; Ghimire et al., 2014). At present, g_c is usually calculated from the inverted Penman–Monteith (PM) equation based on data with sap flow method (Monteith, 1981; Granier et al., 2000a; Fernández et al., 2009; Kochendorfer et al., 2011; Ghimire et al., 2014). Sap flow method can provide direct and robust means of continuous measurement of water flux from trees (Granier et al., 1996, 2000a; Tang et al., 2006; Herbst et al., 2007, 2008; Nadezhdina et al., 2007, 2012), and provide mechanistic details on physiological and environmental controls of transpiration at the branch and whole plant level (Wilson et al., 2001). It is also well suited for determining species effects and other types of variability that occur in highly heterogeneous environments (Wullschleger et al., 2000; Wilson et al., 2001; Chang et al., 2014). Furthermore, measured sap flow data has been used successfully to derive values of g_c for varied vegetation

* Corresponding author at: Tianshui Road 222, Lanzhou, Gansu Province 730000, China.
E-mail address: zhugf@lzu.edu.cn (G. Zhu).

http://dx.doi.org/10.1016/j.agrformet.2015.08.267
0168-1923/

types (Wullschleger et al., 2000; Motzer et al., 2005; Komatsu et al., 2012; Ghimire et al., 2014; Liu et al., 2015), and helps to understand g_c in regulating E_c in response to environmental condition changes (Ghimire et al., 2014). However, previous studies were mainly conducted in forest ecosystems (Oren et al., 1999, 2001; Ewers et al., 2005; Herbst et al., 2007, 2008; Fernández et al., 2009), detailed studies of fruit trees in oasis farmland ecosystems are relatively rare or nonexistent.

Canopy conductance (g_c) responds to multiple environmental variables (Damour et al., 2010). Previous studies often use midday data to quantify and simulate the responses of g_c to its influencing factors (Irvine et al., 2004; Herbst et al., 2008; Fernández et al., 2009; Kochendorfer et al., 2011; Zhang et al., 2012; Zhu et al., 2013; Hirano et al., 2014), morning and afternoon data were usually eliminated from their procedure due to low values in global radiation (R), vapor pressure deficit (D) or E_c (Granier et al., 2000b). Most studies found that g_c decreased with increasing D, and the relationship generally followed an exponential decay (Cienciala et al., 1992; Monteith and Unsworth, 1990; Oren et al., 1999; Motzer et al., 2005; Chang et al., 2006, 2014; Tang et al., 2006). While recently, Liu et al. (2015) reported that g_c was positively linear with D in a banana plantation in Northern Israel. Thus, the responses of g_c to environmental factors for different ecosystems still need to be carefully investigated, and it is urgent to catch a whole-day picture of the relationships between g_c and environmental factors.

Based on sap flow measurements and related micrometeorological and biological variables (i.e. leaf dimension, leaf area and leaf area index) in two study years, the specific objectives of this study were (1) to clarify diurnal courses of E_c and g_c of the vine canopy; (2) to examine relationships among E_c, g_c and main meteorological variables; (3) to quantify and model the daytime variations in g_c. By estimating the responses of g_c to main meteorological variables, this study is aimed to improve our understanding of the feed backs between the planted land surface and the atmosphere in the oasis farmland ecosystem.

2. Materials and methods

2.1. Site description

The experiment was conducted in Nanhu Oasis, Danghe river basin, Gansu Province, China (39°52′34″ N, 94°06′19″ E; 1300 m a.s.l), which belongs to a typical continental temperate zone. The study area has flat terrain, abundant sunlight with the annual total radiation between 5903.4 and 6309.5 MW m^{-2}, and convenient water resources from Wowa Lake, which is less than 2 km in the southeast. The annual average temperature and precipitation is 9.3 °C and 36.9 mm, respectively. The annual potential evapotranspiration is around 2400 mm (Ma et al., 2013). The soil type is Arenosols according to FAO classification, with a mean soil bulk density being 1.41 g cm^{-3}.

One vine plot (450 m × 160 m) was selected in the oasis to conduct our study. *Vitis vinifera* L. (cv. Thompson Seedless) grapevines were planted in rows at a spacing of 1 m between vines and 3 m between rows oriented north–south. The shoots were maintained on a vertical plane by three wires supported by a 2.5 m high T-trellis system. The root depth of the vines was about 1.0 m below the surface, which had no access to groundwater. The vineyard was furrow-irrigated every month during the growing seasons.

2.2. Environmental conditions and biological factors observation

Weather conditions were continuously monitored by an automatic weather station on site during the two study years. Rainfall was monitored by a tipping bucket rain gauge (TE525, Texas Electronics, USA). Global radiation (NR01, Hukseflux, Netherland) were measured at heights of 3 m above the ground. Both air temperature and relative humidity (HMP60, Vaisala, Finland) were measured at heights of 1, 1.5, 2, 2.5 and 3 m above the ground. Wind speed/direction (5103, R. M. Young, USA) were monitored about 0.5 m above the canopy. Soil water content (ML2x, Delta T, UK) was measured at 0.05, 0.1, 0.2, 0.5, 0.8 and 1 m depths. Half-hourly averages of the above data were computed and stored on a data logger (CR1000, Campbell, USA).

Leaf area index (*LAI*, LAI-2200, Li-Cor, USA) and leaf area were measured every 15 days on site. An allometric relationship between leaf length (cm), leaf width (cm) and leaf area (cm^2) was obtained (leaf area = 0.70 × leaf length × leaf width + 2.57, r^2 = 0.99), with the measurements of 150 leaves collected from the yard. Total leaf area (A, m^2) for each sample vine was then determined every month with measurements of all leaves. The average A showed narrow variation during study periods in two years, with values of about 3.62 ± 0.10 m^2 in 2013, and 3.65 ± 0.14 m^2 in 2014, respectively. Details about leaf area observation can be seen in Supplement.

2.3. Sap flow measurements

Six representative vines were selected every year with trunk diameters ranging from 1.97 to 4.14 cm, which covered most diameters of the vines in the yard. The heat balance method (Sakuratani, 1981) was used to measure sap flow (F, g h^{-1}) of grapevine with the Dynagage Flow 32A system (Dynamax, Houston, USA). To avoid water damage during irrigation, the gauges were installed at the height of more than 40 cm above the ground on trunk per vine. Details of the theory and installation can be seen in peers' work (Trambouze and Voltz, 2001). Gauge outputs were measured every 60 s and recorded as 30-min averages with a data logger (CR1000, Campbell, USA). Sap flow measurements were made between July 19 (DOY 200) and September 15 (DOY 258) in 2013, and between July 23 (DOY 204) and September 17 (DOY 260) in 2014.

2.4. Canopy transpiration (E_c) and canopy conductance (g_c)

Half-hourly canopy transpiration (E_c, mm h^{-1}) was calculated as (Soegaard and Boegh, 1995; Zhang et al., 2011):

$$E_c = \frac{k}{N}\sum_{i=1}^{N}\frac{F_i}{A_i} \times LAI \quad (1)$$

where k is used for units conversion (k = 0.001); N is the sampling number; F_i is sap flow of the ith individual (g h^{-1}); A_i is leaf area of the ith individual (m^2).

When calculating canopy conductance (g_c, mm s^{-1}), periods of rainfall and data obtained under the conditions of R < 0 and D < 0.5 kPa were excluded (Ewers and Oren, 2000). This is mainly because when R, D, and sap flow were close to zero, it will increase the relative inaccuracy in g_c calculation (Granier et al., 2000a). Half-hourly g_c was then calculated from E_c and meteorological data with the simplified PM equation (Monteith and Unsworth, 1990):

$$g_c = \frac{\lambda(T)E_c\gamma(T)}{\rho(T)C_pD} \quad (2)$$

where $\gamma(T)$ is the psychometric constant as a function of temperature (T, °C) (Pa K^{-1}), $\lambda(T)$ is the latent heat of vaporization of water (J kg^{-1}), E_c is transpiration (kg m^{-2} s^{-1}), C_p is the specific heat of air (J kg^{-1} K^{-1}), $\rho(T)$ is the density of liquid water (kg m^{-3}), and D is the vapor pressure deficit (Pa).

This equation could be applied based on the assumption that the studied canopy was well coupled aerodynamically (Phillips and Oren, 1998). To address this assumption, aerodynamic conductance (g_a, mm s^{-1}) was estimated according to Thom and Oliver

(1977), and the dimensionless decoupling factor (Ω) was also estimated according to Jarvis and McNaughton (1986). During two study years, g_a ranged from 36.1 mm s^{-1} to 124.7 mm s^{-1} with a mean of 46.4 mm s^{-1}, and daytime mean Ω was 0.18 (unpublished data). The low values of Ω indicated that our vineyard was well coupled to the atmosphere, and Eq. (2) was applicable for calculating g_c values.

2.5. Modeling canopy conductance (g_c)

The whole daytime was divided into three time periods, including the first period (7:00–11:00), the second period (11:00–17:00) and the third period (17:00–21:00). Then the responses of g_c to main micrometeorological variables in each time period were simulated separately.

The responses of g_c in the first period and third period were modeled using the simple linear model as follows, where a, b, c and d are parameters to be fitted:

$$g_c = a \times R + b \times T + c \times D + d \quad (3)$$

The responses of g_c in the second period were formulated using a series of multiplicative functions (Jarvis, 1976; Stewart, 1988). Due to the small range of T and unlimited soil water content, g_c in the second period was modeled using the negative logarithmic equation as follows (Granier et al., 2000b), where a, b, c and d are parameters to be fitted:

$$g_c = \left[\frac{R}{(R+a)}\right] \times (b - c \ln D) \quad (4)$$

2.6. Cross-validation of models

To validate the selected models above (Eqs. (3) and (4)), the selected models were fitted separately to year 2013 and 2014, and then cross-validated on each other (Stewart, 1988). The fitted models for each year were used to predict the values of g_c for the other year, and the relationships between measured g_c and predicted g_c were examined.

3. Results

3.1. Environmental and biological factors

Daily variations of environmental and biological factors during study periods in 2013 and 2014 are shown in Fig. 1, including mean daytime global radiation (R), mean daily air temperature (T), mean daytime vapor pressure deficit (D), mean daily wind speed (u), daily

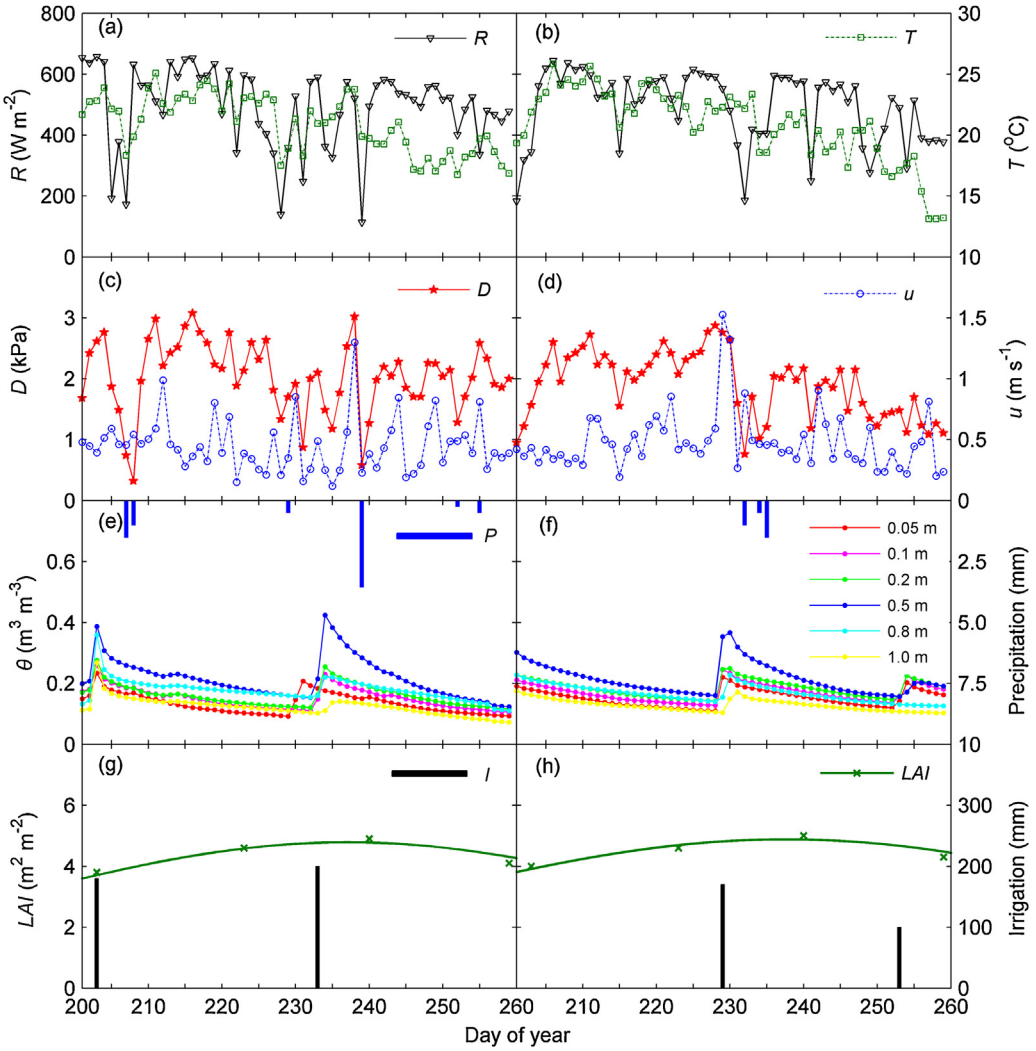

Fig. 1. Environmental and biological factors during the 2013 (a, c, e, g) and 2014 (b, d, f, h) study periods, include mean daytime global radiation (R), mean daily air temperature (T), mean daytime vapor pressure deficit (D), mean daily wind speed (u), daily soil water content (θ) at 0.05, 0.1, 0.2, 0.5, 0.8, and 1 m depth, daily precipitation (P), leaf area index (LAI) and irrigation amounts (I).

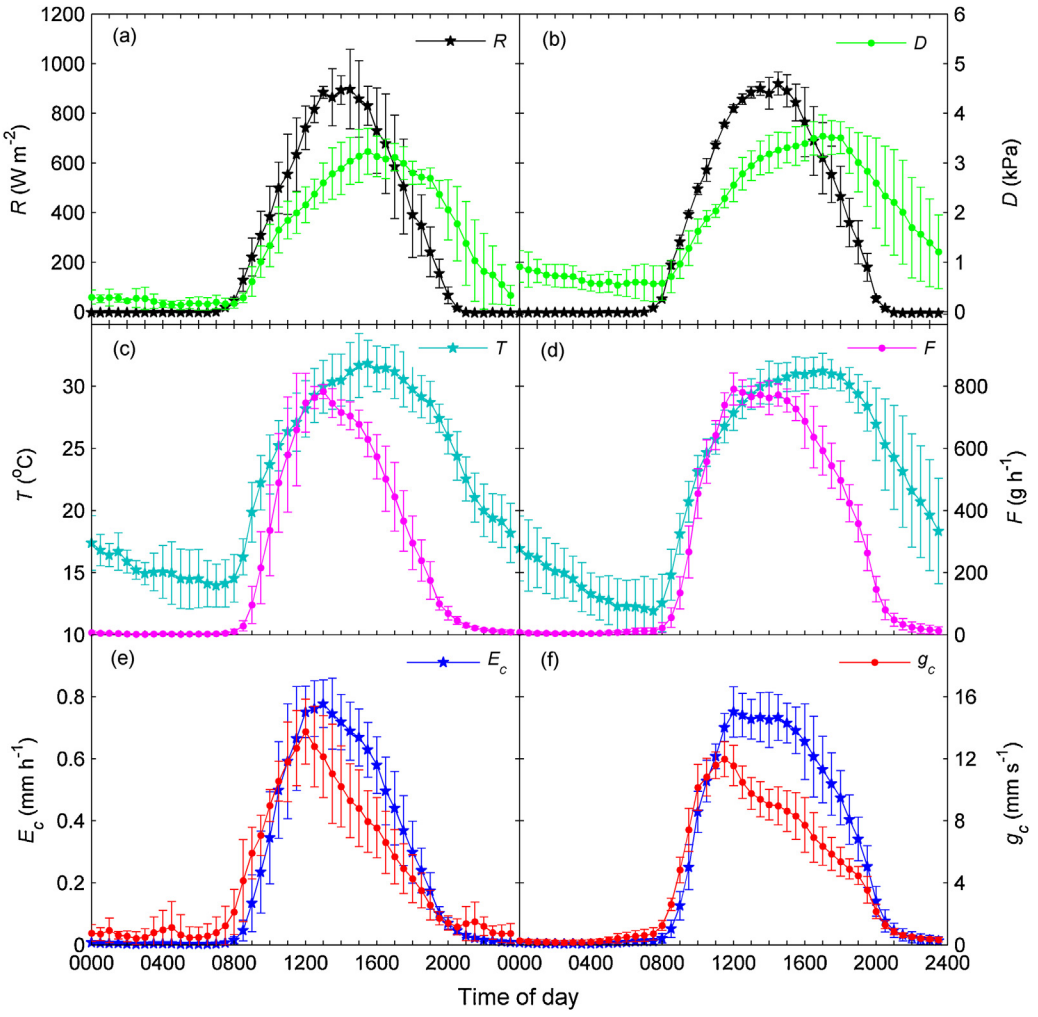

Fig. 2. Mean diurnal courses of global radiation (R), vapor pressure deficit (D), air temperature (T), mean sap flow (F), canopy transpiration (E_c) and canopy conductance (g_c) in 7 bright days in 2013 (a, c, e, DOY 223–232) and 2014 (b, d, f, DOY 222–231) study periods. The bars represent the standard deviations about the mean.

soil water content (θ) at 0.05, 0.1, 0.2, 0.5, 0.8 and 1 m depth, daily precipitation (P), leaf area index (LAI) and irrigation amounts (I). There were no significant inter-annual differences in two study years (Fig. 1). During study periods in two years, the mean daytime R varied from 113.7 to 657.2 W m^{-2} with an average value of 492.8 W m^{-2} (Fig. 1a and b). The variation of mean daily T has a similar trend to R, varying from 13.1 to 25.9 °C with a mean value of 20.9 °C (Fig. 1a and b). The mean daytime D exhibited large daily variation ranging from 0.3 to 3.1 kPa with a mean value of 2.0 kPa (Fig. 1c and d). Daily mean u ranged from 0.1 to 1.5 m s^{-1} (Fig. 1c and d). Total precipitation was both less than 5.0 mm during the whole study periods in two study years (Fig. 1e and f). Variability of θ mainly depended on local irrigation scheduling (Fig. 1e and f). After irrigation, θ reached its peak value (about 0.4 m^3 m^{-3}) and gradually decreased until the next irrigation. The LAI showed narrow variation during two study periods with the average values of about 4.5 m^2 m^{-2} in 2013, and 4.4 m^2 m^{-2} in 2014 (Fig. 1g and h).

3.2. *Diurnal courses of micrometeorological variables,* F, E_c *and* g_c

The mean diurnal courses of micrometeorological variables, F, E_c and g_c during two study years are showed in Fig. 2 All variables exhibited single peak curves throughout the day and showed no significant inter-annual variations. As is shown in Fig. 2, R increased quickly between 7:00 and 8:00, and reached peak values about 1000 W m^{-2} between 13:00 and 14:00, then declined rapidly and dropped to near zero between 21:00 and 22:00 (Fig. 2a and b). D increased along with R in the morning, and arrived at the maximum values of about 3.5 kPa between 16:00 and 17:00, then declined sharply until next morning (Fig. 2a and b). T varied synchronously with D, which began to increase between 7:00 and 8:00, and arrived at the maximum values of about 33 °C between 16:00 and 17:00, then declined sharply until next morning (Fig. 2c and d). Diurnal courses of F (Fig. 2c and d) and E_c (Fig. 2e and f) had a similar trend, which increased quickly in the morning, and reached peak values about 800 g h^{-1} and 0.8 mm h^{-1} between 13:00 and 14:00, then declined rapidly and dropped to near zero between 21:00 and 22:00. Complete diurnal patterns of g_c were observed in two study years, which began to increase between 7:00 and 8:00, reached the maximum values of about 14 mm s^{-1} between 11:00 and 12:00, then decreased gradually to zero between 21:00 and 22:00 (Fig. 2e and f).

3.3. *Hysteresis loops between* g_c *and main micrometeorological variables*

Hysteresis loops were observed between g_c and main micrometeorological variables during two study years (Fig. 3). The direction of the loops tracked clockwise for R, D and T. In order to reveal the main influencing factors on g_c in different daytime periods, the relationships between g_c and single meteorological factor were conducted. It was observed that g_c responded positively to R, D and

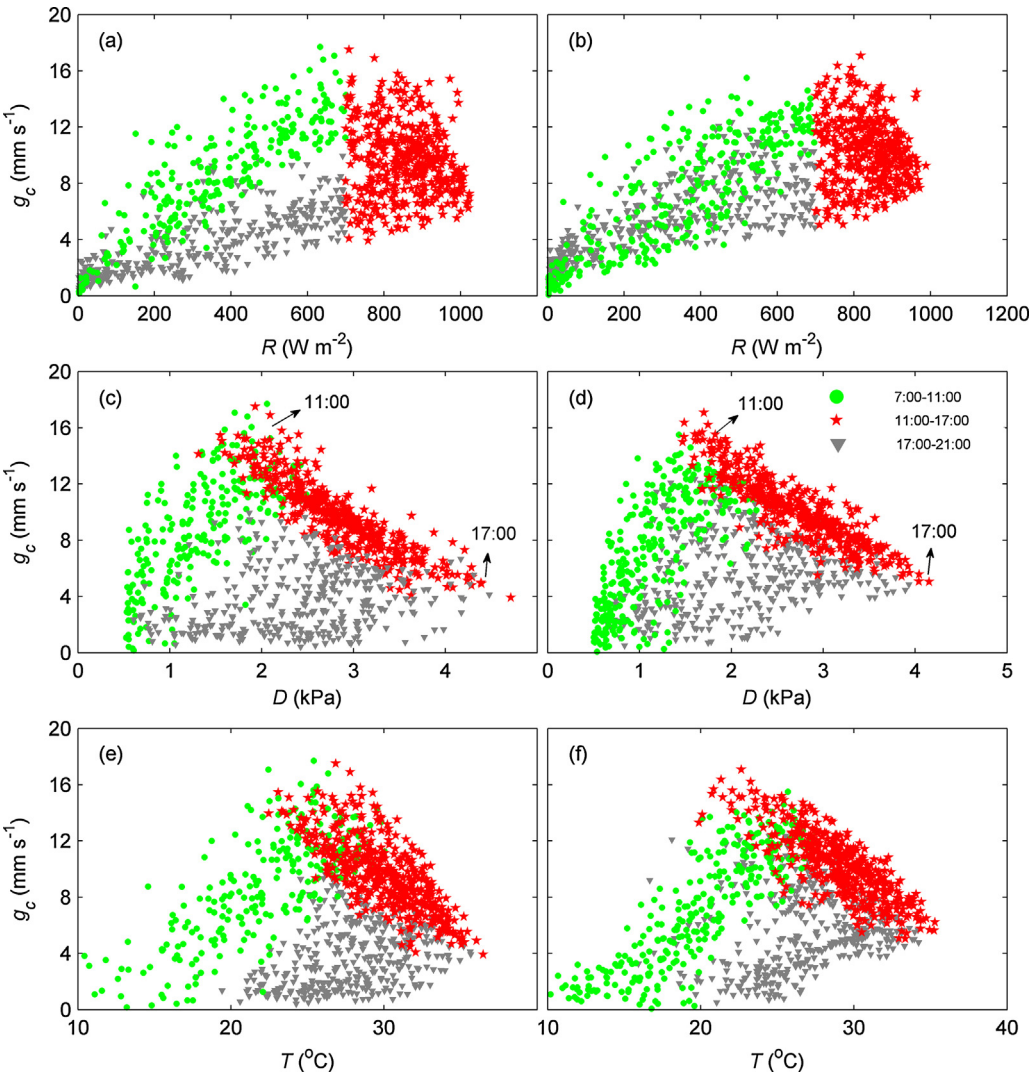

Fig. 3. Hysteresis loops between g_c and main micrometeorological variables (R, D, T) in entire rainless days during the 2013 (a, c, e) and 2014 (b, d, f) study periods.

Table 1
Single factor regressions between canopy conductance (g_c) and global radiation (R), air temperature (T) and vapor pressure deficit (D) in different daytime periods, r was the correlation coefficient.

Factor	Year 2013 (DOY 200–258)		Year 2014 (DOY 204–260)	
	Regression equation	r^2	Regression equation	r^2
The first period (7:00–11:00)				
R	$g_c = (1.78 \times 10^{-2}) \times R + 2.08$	**0.75**	$g_c = (1.68 \times 10^{-2}) \times R + 1.35$	**0.70**
D	$g_c = 7.70 \times D - 1.62$	**0.51**	$g_c = 6.50 \times D - 0.28$	**0.53**
T	$g_c = 0.67 \times T - 6.14$	**0.56**	$g_c = 0.81 \times T - 9.15$	**0.72**
The second period (11:00–17:00)				
R	$g_c = (-4.62 \times 10^{-3}) \times R + 13.60$	0.02	$g_c = (-4.67 \times 10^{-3}) \times R + 14.11$	0.02
D	$g_c = 30.48 \times \exp(-0.41 \times D)$	**0.79**	$g_c = 27.34 \times \exp(-0.37 \times D)$	**0.79**
T	$g_c = -0.70 \times T + 30.69$	**0.54**	$g_c = -0.67 \times T + 29.69$	**0.65**
The third period (17:00–21:00)				
R	$g_c = (0.77 \times 10^{-3}) \times R + 1.30$	**0.60**	$g_c = (0.93 \times 10^{-3}) \times R + 2.57$	**0.58**
D	$g_c = 0.66 \times D + 2.20$	0.05	$g_c = 1.20 \times D + 2.20$	0.05
T	$g_c = 0.20 \times T - 1.79$	0.09	$g_c = 0.30 \times T - 3.00$	0.02

The bold number means that the correlation coefficient (r^2) is higher than 0.50.

T in the first (7:00–11:00) and third (17:00–21:00) periods, but negatively in the second period (11:00–17:00) (Table 1). Relationships between E_c and main meteorological variables during two study years are also plotted in Fig. 4. During a whole day, E_c was linearly correlated with R ($r^2 = 0.85$ in 2013, 0.88 in 2014). Although the relationships between E_c and D and T also exhibited hysteresis loops, they had relatively less regularities compared with the hysteresis loops between g_c and D and T (Fig. 4).

3.4. Modeling g_c

Based on the results of single factor regression analysis, diurnal variations in g_c were modeled by using the linear model (Eq. (3)) for the first and third periods and the negative logarithmic model (Eq. (4)) for the second period. The fitted values of the parameters are showed in Table 2. For the first and third periods, the fitted linear models explained more than 73% of the variations in g_c ($r^2 = 0.78$

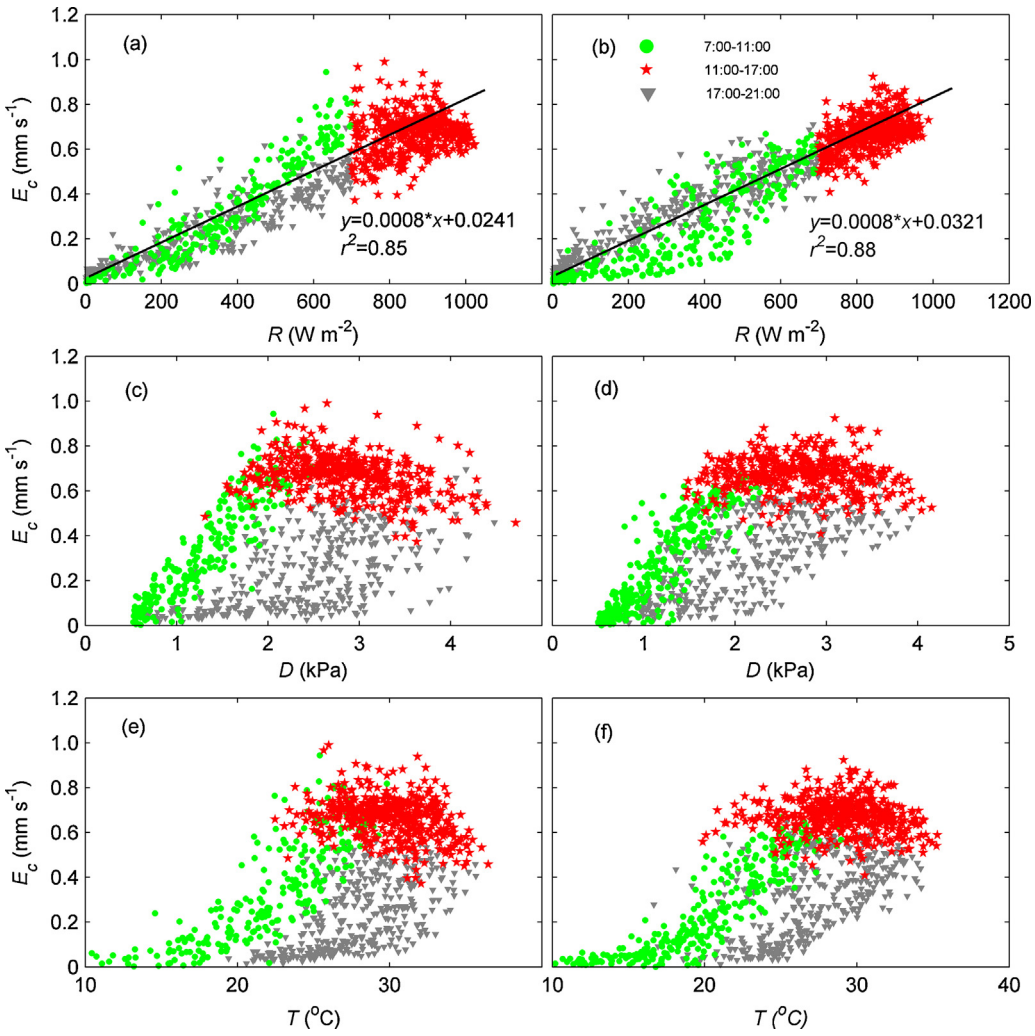

Fig. 4. Relationships between E_c and main micrometeorological variables (R, D, T) in entire rainless days during the 2013 (a, c, e) and 2014 (b, d, f) study periods.

Table 2
Fitted values of parameters for simple linear and negative logarithmic models relating canopy conductance (g_c) to global radiation (R), air temperature (T) and vapor pressure deficit (D). Parameters a, b, c and d were obtained by fitting the modified negative logarithmic and simple linear models (Eqs. (3) and (4)), r was the correlation coefficient, *RMSE* was the root mean square error.

Parameter	All data	Year 2013 (DOY 200–258)	Year 2014 (DOY 204–260)
$g_c = a \times R + b \times T + c \times D + d$: The first period (7:00–11:00)			
a	1.33×10^{-2}	2.14×10^{-2}	1.04×10^{-2}
b	−2.00	−3.05	−1.96
c	0.46	0.20	0.59
d	−4.02	0.37	−5.94
r^2	0.77	0.78	0.80
RMSE	1.96	1.85	1.86
$g_c = [R/R + a](b - c \ln D)$: The second period (11:00–17:00)			
a	7.72×10^2	4.16×10^2	1.66×10^3
b	40.63	31.98	62.91
c	21.53	17.07	33.24
r^2	0.82	0.80	0.84
RMSE	1.07	1.14	0.98
$g_c = a \times R + b \times T + c \times D + d$: The third period (17:00–21:00)			
a	1.30×10^{-2}	1.11×10^{-2}	1.36×10^{-2}
b	−1.21	−0.68	−1.35
c	−0.18	−0.19	−0.14
d	8.12	6.99	7.80
r^2	0.70	0.73	0.74
RMSE	1.45	1.17	1.38

and 0.73 respectively for the first and third periods in 2013, and 0.80 and 0.74, respectively, for the first and third periods in 2014). These indicated that g_c in these two periods can be well modeled by the combinations of the three variables. For the second period, the negative logarithmic models can explained more than 80% of the variations in g_c (r^2 = 0.80 and 0.84, for 2013 and 2014, respectively). Due to the narrow range of T in this period and the dependence of D on T, adding T as a third predictor to the negative logarithmic model produced no significant improvement. Thus, only D and R could be used as predictors to produce satisfactory simulation results.

The results of cross-validation of the selected models are showed in Fig. 5 For the first period (Fig. 5a and b), the regression slopes between measured and predicted g_c were 0.81 and 0.82 with r^2 = 0.70 and 0.72 for 2013 and 2014, respectively. For the second period (Fig. 5c and d), the regression slopes between measured and predicted g_c were 0.76 and 0.88 with r^2 = 0.71 and 0.82 for 2013 and 2014, respectively. The points between measured and predicted g_c were located around the 1:1 line (Fig. 5c and d), indicating that there were no significant inter-annual variability in g_c during this period of two study years. For the third period (Fig. 5e and f), however, the points were mostly on one side of the line of equality. The predicted g_c values were higher than measured values in 2013 (with regression slope being 0.88 and r^2 = 0.72), but lower in 2014 (with regression slope being 0.62 and r^2 = 0.74). Overall, the proposed models were reasonably precise and exhibited slightly inter-annual variability in predicting variations in g_c in this study.

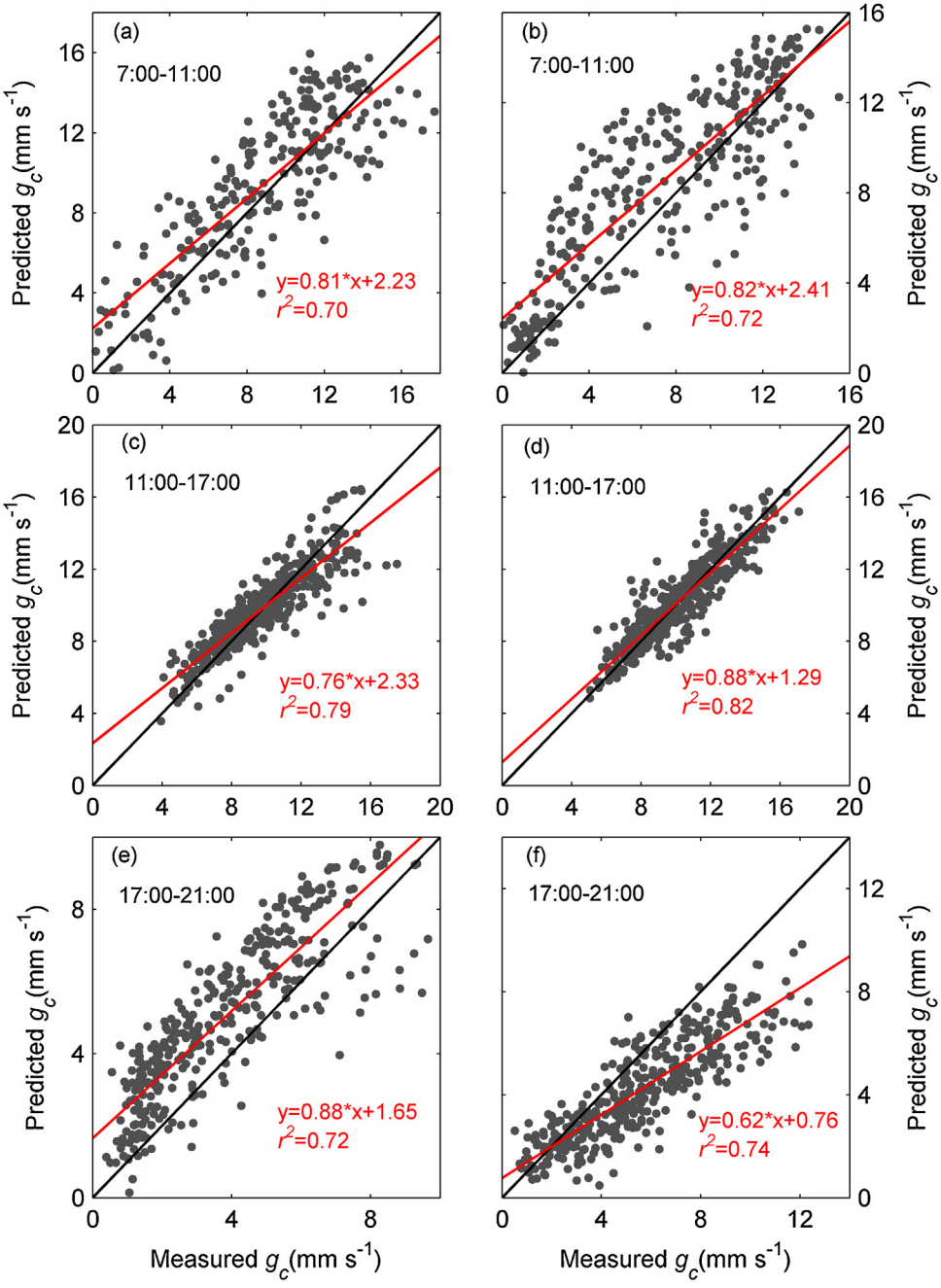

Fig. 5. Relationships between predicted and measured g_c. Models were cross-validated on the 2013 (a, c, e) and 2014 (b, d, f) study periods. The red line on each graph represents the regression line and the blank line represents the 1:1 line between predicted and measured values. (For interpretation of the references to color in this figure legend, the reader is referred to the web version of this article.)

4. Discussion

4.1. Relationships between g_c and micrometeorological variables

Although relationships between g_c and micrometeorological variables have been widely discussed in recent years (for a review, see Damour et al., 2010), the whole-day pattern of the variations in g_c and the relationships between g_c and micrometeorological variables still remain unclear. Most previous studies found that g_c was mainly controlled by D, and g_c generally decreased exponentially with increasing D (i.e. Cienciala et al., 1992; Fernández et al., 2009; Komatsu et al., 2012). Recently, Chang et al. (2014) found an exponential decay between D and g_c in a *Picea crassifolia* stand in a natural forest, for which D accounted for 81% variations in g_c. Ghimire et al. (2014) reported that the inverse relationship between g_c and D explained most of the variations in g_c for a natural broad-leaved forest and a mature planted pine forest. Some studies reported that g_c was controlled by both R and D. For example, Motzer et al. (2005) reported that R and D were the major environmental determinants of g_c in a lower tropical Montane rain forest. Liu et al. (2015) reported that g_c was positively linearly with both D and R in a banana plantation in Northern Israel. Previous studies reported T was also an important influencing factor on g_c, while their relationships varied in different studies. For example, Granier et al. (2000a) reported a linear relationship between g_c and T below 17 °C in a young beech stand. Lagergren and Lindroth (2002) found that inclusion of a linear or exponential function for T improved the g_c model for pine.

In our study, it was observed that the responses of g_c to micrometeorological variables and the controlling factors of g_c were significantly different during different daytime periods. The results were also helpful in better understanding the bulk behavior of stomata in response to changing environmental conditions (Ghimire et al., 2014). In the first period, stomatal opened quickly as R, D and T increase (Jones, 2014), so g_c increased positively to increasing R, D and T, and each of them had a significant correlation with g_c ($r^2 > 0.50$; Table 1). In the second period, stomatal closure avoided excessive water loss and prevented leaf water potential from falling to a dangerous level (Lu et al., 2003), so g_c decreased negatively to increasing R, D and T, and the primary factors controlling g_c were D and T ($r^2 > 0.55$; Table 1). The values of D at which g_c began to decline were about 2 kPa, which were higher than 1 kPa for some forest species (Ewers et al., 2005; Herbst et al., 2007, 2008). In the third period, as stomatal aperture kept decreasing until sunset, g_c decreased positively to decreasing R, D and T (Mallick et al., 2013), and R was the primary factor controlling g_c ($r^2 > 0.58$; Table 1). Noticeably, the slopes of regression equations in the first period were significantly higher than the third period (Table 1 and Fig. 3), indicating that the morning g_c was more sensitive to environmental factors than the afternoon g_c. This may be due to the higher hydraulic resistance of the vine during the afternoon than that during the morning (Fernández et al., 2009).

4.2. Hysteresis loops between g_c and main micrometeorological variables

The different responses of g_c to main micrometeorological variables during three time periods formed the hysteresis loops during the daytime. These loops were also observed at different stages of the vine growth and development, and they exhibited a significant seasonal variation (see details in the Supplement). Thus, it may not be appropriate to pull the whole-day data of g_c and environmental variables together for statistical analysis. Instead, the changes in g_c should be analyzed separately during different daytime periods to investigate the relationships between g_c and environmental variables. This may be useful to improve our current understanding of the relationships between the plant physiological and environmental processes. The results could be used to fine-tune g_c and E_c modeling in vine plantations in oasis ecosystem. So far, a few studies demonstrated the existence of hysteresis loops between g_c (or E_c) and meteorological variables. For example, Ewers et al. (2005) found hysteresis loops between E_c and D and photosynthetically active radiation (Q_o) for boreal forest stands. However, they did not observe loops between g_c and D and Q_o. Fernández et al. (2009) found loops between g_c and D in both exotic species (*P. menziesii*) and native species (*N. antarctica*, *L. hirsuta*, *S. patagonicus* and *D. juncea*). Jones (2014) reported that the stomatal light-response curves for *Pinus sylvestris* illustrate the hysteresis that can occur in certain conditions. Liu et al. (2015) found that the relationship between g_c and D exhibited hysteresis loops in a banana plantation in Northern Israel.

For the purpose of modeling g_c, the Jarvis-type multiplicative model (Jarvis, 1976; Stewart, 1988) was commonly used (Granier et al., 2000a, 2000b; Tang et al., 2006; Quentin et al., 2011; Wang et al., 2014). The Jarvis-type model generally relates the variations in g_c to a number of environmental variables (i.e. T, D, R, θ, CO_2 concentration, and leaf water potential). However, so many input variables hardly make it practical. Granier et al. (1996) used a simplified Jarvis-type model to simulate g_c in relation to R and D for a sessile oak stand, over a period of nonlimiting soil water content, of maximal *LAI* and in dry canopy conditions. Here, the similar simplified model was also used to simulate the variations in g_c in the second period, and a simple linear model for the first and third period. These models when combined were precise and reliable in predicting the whole daytime variations in g_c. However, all these approaches were the products of the response functions to several influencing factors, and were essentially empirical and require new parameterization for new environmental conditions (Damour et al., 2010). Thus, the applicability of our predictive schemes may be limited to the mature period of the oasis farmland ecosystem.

5. Conclusions

This study investigated diurnal patterns of g_c during two study years for a vineyard at an oasis in Northwest China, and found that the relationships between g_c and main micrometeorological variables during the day exhibited hysteresis loops. It was found that g_c responded positively to R, D and T in the first period (7:00–11:00) and third (17:00–21:00) period, but negatively in the second period (11:00–17:00). The results showed that the responses of g_c to micrometeorological variables were significantly different during different daytime periods. A simple linear model was used to simulate variations in g_c for the first period and the third period, and a negative logarithmic model for the second period. These models were consistent in predicting the whole daytime variations in g_c in two study years.

In the future, it is important to conduct fundamental and systematical studies to get a more comprehensive and mechanistic understanding of the temporal trends in g_c at different stages of the vine growth and development, and develop predictive g_c and E_c models for vine plantations in the oasis ecosystem.

Acknowledgements

We would like to thank Timo Vesala (Associate Editor) for his continuous help during the review process and thank the anonymous reviewers for their critical reviews and helpful comments on the draft of the manuscript. This research was supported by National Key Scientific Research Projects (973) (No. 2013CB956604), the Chinese Academy of Sciences Action Plan for West Development Program Project (KZCX2-XB3-15), National Natural Science Foundation of China (Nos. 41571016, 31370467 and 41271359).

Appendix A. Supplementary data

Supplementary material related to this article can be found, in the online version, at http://dx.doi.org/10.1016/j.agrformet.2015.08.267.

References

Alfieri, J.G., Niyogi, D., Blanken, P.D., Chen, F., LeMone, M.A., Mitchell, K.E., Ek, M.B., Kumar, A., 2008. Estimation of the minimum canopy resistance for croplands and grasslands using data from the 2002 International H_2O Project. Mon. Weather Rev. 136 (11), 4452–4469.

Berry, J., Beerling, D., Franks, P., 2010. Stomata: key players in the earth system, past and present. Curr. Opin. Plant Biol. 13, 232–239.

Buckley, T.N., Turnbull, T.L., Adams, M.A., 2012. Simple models for stomatal conductance derived from a process model: cross-validation against sap flux data. Plant Cell Environ. 35, 1647–1662.

Chang, X., Zhao, W., Zhang, Z., Su, Y., 2006. Sap flow and tree conductance of shelter-belt in arid region of China. Agric. For. Meteorol. 138, 132–141.

Chang, X., Zhao, W., Liu, H., Wei, X., Liu, B., Liu, Z., 2014. Qinghai spruce (*Picea crassifolia*) forest transpiration and canopy conductance in the upper Heihe River Basin of arid northwestern China. Agric. For. Meteorol. 198–199, 209–220.

Cienciala, E., Lindroth, A., Èermák, J., Hallgren, J.E., Kuèera, J., 1992. Assessment of transpiration estimates for *Picea abies* trees during a growing season. Trees Struct. Funct. 6, 121–127.

Daly, E., Porporato, A., Rodriguez-Iturbe, I., 2004. Coupled dynamics of photosynthesis, transpiration, and soil water balance. Part I. Upscaling from hourly to daily level. J. Hydrometeorol. 5, 546–558.

Damour, G., Simonneau, T., Cochard, H., Urban, L., 2010. An overview of models of stomatal conductance at the leaf level. Plant Cell Environ. 33 (9), 1419–1438.

Ewers, B.E., Gower, S.T., Bond-Lamberty, B., Wang, C.K., 2005. Effects of stand age and tree species on canopy transpiration and average stomatal conductance of boreal forests. Plant Cell Environ. 28 (5), 660–678.
Ewers, B.E., Oren, R., 2000. Analyses of assumptions and errors in the calculation of stomatal conductance from sap flux measurements. Tree Physiol. 20 (9), 579–589.
Fernández, M.E., Gyenge, J., Schlichter, T., 2009. Water flux and canopy conductance of natural versus planted forests in Patagonia, South America. Trees Struct. Funct. 23 (2), 415–427.
Ghimire, C.P., Lubczynski, M.W., Bruijnzeel, L.A., Chavarro-Rincón, D., 2014. Transpiration and canopy conductance of two contrasting forest types in the Lesser Himalaya of Central Nepal. Agric. For. Meteorol. 197, 76–90.
Granier, A., Biron, B., Lemoine, D., 2000a. Water balance, transpiration and canopy conductance in two beech stands. Agric. For. Meteorol. 100, 291–308.
Granier, A., Huc, R., Barigah, S.T., 1996. Transpiration of natural rain forest and its dependence on climatic factors. Agric. For. Meteorol. 100, 291–308.
Granier, A., Loustau, D., Breda, N., 2000b. A generic model of forest canopy conductance dependent on climate, soil water availability and leaf area index. Ann. Forest Sci. 57, 755–765.
Herbst, M., Roberts, J.M., Rosier, P.T.W., Gowing, D.J., 2007. Seasonal and interannual variability of canopy transpiration of a hedgerow in southern England. Tree Physiol. 27, 321–333.
Herbst, M., Rosier, P.T.W., Morecroft, M.D., Gowing, D.J., 2008. Comparative measurements of transpiration and canopy conductance in two mixed deciduous woodlands differing in structure and species composition. Tree Physiol. 28, 959–970.
Hirano, T., Kusin, K., Limin, S., Osaki, M., 2014. Evapotranspiration of tropical peat swamp forests. Glob. Change Biol., http://dx.doi.org/10.1111/gcb.12653.
Irvine, J., Law, B.E., Kurpius, M.R., Anthoni, P.M., Moore, D., Schwarz, P.A., 2004. Age-related changes in ecosystem structure and function and effects on water and carbon exchange in ponderosa pine. Tree Physiol. 24, 753–763.
Jarvis, P.G., 1976. The interpretation of the variations in leaf water potential and stomatal conductance found in canopies in the field. Philos. Trans. R. Soc. B 273 (927), 593–610.
Jarvis, P.G., McNaughton, K.G., 1986. Stomatal control of transpiration: scaling up from leaf to region. Adv. Ecol. Res. 15, 1–49.
Jasechko, S., Sharp, Z.D., Gibson, J.J., Birks, S.J., Yi, Y., Fawcett, P.J., 2013. Terrestrial water fluxes dominated by transpiration. Nature 496 (7445), 347–350.
Jones, H.G., 2014. Plant and Microclimate: A Quantitative Approach to Environmental Plant Physiology, 3rd ed. Cambridge University Press, UK, pp. 135–144.
Kochendorfer, J., Castillo, E.G., Haas, E., Oechel, W.C., Kyaw, T.P.U., 2011. Net ecosystem exchange, evapotranspiration and canopy conductance in a riparian forest. Agric. For. Meteorol. 151, 544–553.
Komatsu, H., Onozawa, Y., Kume, T., Tsuruta, K., Shinohara, Y., Otsuki, K., 2012. Canopy conductance for a Moso bamboo (*Phyllostachys pubescens*) forest in western Japan. Agric. For. Meteorol. 156, 111–120.
Kumar, A., Chen, F., Niyogi, D., Alfieri, J.G., Ek, M., Mitchell, K., 2011. Evaluation of a photosynthesis-based canopy resistance formulation in the Noah land-surface model. Bound.-Layer Meteorol. 138, 263–284.
Lagergren, F., Lindroth, A., 2002. Transpiration response to soil moisture in pine and spruce trees in Sweden. Agric. For. Meteorol. 112 (2), 67–85.
Liu, H., Cohen, S., Lemcoff, J.H., Israeli, Y., Tanny, J., 2015. Sap flow, canopy conductance and microclimate in a banana screenhouse. Agric. For. Meteorol. 201, 165–175.
Lu, P., Yunusa, I.A.M., Walker, R.R., Muller, W.J., 2003. Regulation of canopy conductance and transpiration and their modelling in irrigated grapevines. Funct. Plant Biol. 30 (6), 689–698.
Ma, J.Z., He, J.H., Qi, S., Zhu, G.F., Zhao, W., Edmunds, W.M., Zhao, Y.P., 2013. Groundwater recharge and evolution in the Dunhuang Basin, northwestern China. Appl. Geochem. 28, 19–31.
Mallick, K., Jarvis, A., Fisher, J.B., Kenvin, P.T., Boegh, E., Niyogi, D., 2013. Latent heat flux and canopy conductance based on Penman–Monteith Priestley–Taylor equation, and Bouchet's complementary hypothesis. J. Hydrometeorol. 14, 419–442.
Monteith, J.L., Unsworth, M.H., 1990. Principles of Environmental Physics. Edward Arnold, London, pp. 291.
Monteith, J.L., 1981. Evaporation and surface-temperature. Q. J. R. Meteorol. Soc. 107 (451), 1–27.
Motzer, T., Munz, N., Küpper, M., Schmitt, D., Anhuf, D., 2005. Stomatal conductance, transpiration and sap flow of tropical Montane rain forest trees in the southern Ecuadorian Andes. Tree Physiol. 25, 1283–1293.
Nadezhdina, N., Nadezhdin, V., Ferreira, M.I., Pitacco, A., 2007. Variability with xylem depth in sap flow in trunks and branches of mature olive trees. Tree Physiol. 27, 105–111.
Nadezhdina, N., Vandegehuchte, M., Steppe, K., 2012. Sap flux density measurements based on the heat field deformation method. Trees Struct. Funct. 26, 1439–1448.
Ono, K., Maruyama, A., Kuwagata, T., Mano, M., Takimoto, T., Hayashi, K., Hasegawa, T., Miyata, A., 2013. Canopy-scale relationships between stomatal conductance and photosynthesis in irrigated rice. Glob. Change Biol. 19, 2209–2220.
Oren, R., Sperry, J.S., Ewers, B.E., Pataki, D.E., Phillips, N., Megonigal, J.P., 2001. Sensitivity of mean canopy stomatal conductance to vapor pressure deficit in a flooded *Taxodium distichum* L. forest: hydraulic and non-hydraulic effects. Oecologia 126, 21–29.
Oren, R., Sperry, J.S., Katul, G.G., Pataki, D.E., Ewers, B.E., Phillips, N., Schäfer, K.V.R., 1999. Survey and synthesis of intra- and interspecific variation in stomatal sensitivity to vapour pressure deficit. Plant Cell Environ. 22, 1515–1526.
Phillips, N., Oren, R., 1998. A comparison of daily representations of canopy conductance based on two conditional time-averaging methods and the dependence of daily conductance on environmental factors. Ann. Forest Sci. 55 (1–2), 217–235.
Quentin, A.G., O'Grady, A.P., Beadle, C.L., Worledge, D., Pinkard, E.A., 2011. Responses of transpiration and canopy conductance to partial defoliation of *Eucalyptus globulus* trees. Agric. For. Meteorol. 151, 356–364.
Sakuratani, T., 1981. A heat balance method for measuring water flow in the stem of intact plants. J. Agric. Meteorol. 37 (1), 9–17.
Soegaard, H., Boegh, E., 1995. Estimation of evapotranspiration from a millet crop in the Sahel combining sap flow, leaf area index and eddy correlation technique. J. Hydrol. 166, 265–282.
Stewart, J.B., 1988. Modelling surface conductance of pine forest. Agric. For. Meteorol. 43, 19–35.
Tang, J., Bolstad, P.V., Ewers, B.E., Desai, A.R., Davis, K.J., Carey, E.V., 2006. Sap flux-upscaled canopy transpiration, stomatal conductance, and water use efficiency in an old growth forest in the Great Lakes region of the United States. J. Geophys. Res. 111, G02009, http://dx.doi.org/10.1029/2005 JG000083.
Thom, A.S., Oliver, H.R., 1977. On Penman's equation for estimating regional evapotranspiration. Q. J. Roy. Meteor. Soc. 103, 345–357.
Trambouze, W., Voltz, M., 2001. Measurement and modelling of the transpiration of a Mediterranean vineyard. Agric. For. Meteorol. 107 (2), 153–166.
Wang, H., Guan, H., Deng, Z., Simmons, C.T., 2014. Optimization of canopy conductance models from concurrent measurements of sap flow and stem water potential on Drooping Sheoak in South Australia. Water Resour. Res. 50, 6154–6167.
Wilson, K.B., Hanson, P.J., Mulholland, P.J., Baldocchi, D.D., Wullschleger, S.D., 2001. A comparison of methods for determining forest evapotranspiration and its components: sap-flow, soil water budget, eddy covariance and catchment water balance. Agric. For. Meteorol. 106, 153–168.
Wullschleger, S.D., Wilson, K.B., Hanson, P.J., 2000. Environmental control of whole-plant transpiration, canopy conductance and estimates of the decoupling coefficient for large red maple trees. Agric. For. Meteorol. 104, 157–168.
Zhang, Y.J., Meinzer, F.C., Qi, J.H., Goldstein, G., Cao, K.F., 2012. Midday stomatal conductance is more related to stem rather than leaf water status in subtropical deciduous and evergreen broadleaf trees. Plant Cell Environ. 36, 149–158.
Zhang, Y., Kang, S., Ward, E., Ding, R., Zhang, X., Zheng, R., 2011. Evapotranspiration components determined by sap flow and microlysimetry techniques of a vineyard in northwest China: Dynamics and influential factors. Agric. Water Manage. 98, 1207–1214.
Zhu, G., Lu, L., Su, Y., Wang, X., Cui, X., Ma, J., He, J., Zhang, K., Li, C., 2013. Energy flux partitioning and evapotranspiration in a sub-alpine spruce forest ecosystem. Hydrol. Process. 28, 5093–5104.